



Report on Deliverable

Version 5/23/2019	Report on Stability of Laterals	page 1 / 21
-------------------	---------------------------------	-------------

<b>Project</b>	H2020 - SURE (Grant-Number 654662)
<b>Deliverable</b>	D4.3 - Report on Stability of Laterals
<b>Work package</b>	WP4 - Micro-scale
<b>Lead author</b>	Richard Bakker (TU Delft)
<b>Contributor(s)</b>	Christian Kluge (GFZ), Guido Blöcher (GFZ), David Bruhn (TU Delft), Auke Barnhoorn (TU Delft)
<b>Dissemination level</b>	PU (public)
<b>Type</b>	R (document, report)
<b>Due date</b>	February 28 <sup>th</sup> 2018 (M24)
<b>Actual submission date</b>	February 27 <sup>th</sup> 2018
<b>Resubmission date(s)</b>	
<b>Change History</b>	August 6 <sup>th</sup> 2018 - Licence added May 23 <sup>rd</sup> 2019 - DOI and Citation Information added

<b>Licence information</b>	Report D4.3 of the Consortium of the H2020 SURE Project This publication is licensed under a Creative Commons License, International Attribution 4.0: CC BY
<b>DOI (Repository)</b>	10.2312/GFZ.4.8.2019.005
<b>Recommended Citation</b>	Bakker, R.R., Kluge, C., Blöcher, G., Bruhn, D., Barnhoorn, A.; The Horizon 2020 SURE Project: Deliverable 4.3 - Stability of Laterals 2019, Potsdam: GFZ German Research Centre for Geosciences, DOI: 10.2312/GFZ.4.8.2019.005



The SURE project has received funding from the European Union's Horizon 2020 research and innovation programme under grant agreement No 654662.



Version 5/23/2019	Report on Stability of Laterals	page 2 / 21
-------------------	---------------------------------	-------------

Table of Contents

<b>1. Executive Summary .....</b>	<b>3</b>
<b>2. Laboratory Methods .....</b>	<b>3</b>
2.1. Materials .....	3
2.2. $\mu$ CT analysis .....	4
2.3. Acoustic wave speeds .....	5
2.4. Uniaxial Compressive Strength.....	6
2.5. Indirect Tensile Strength and Fracture Toughness tests.....	7
2.6. True-triaxial tests .....	7
<b>3. Results .....</b>	<b>7</b>
3.1. Porosity analysis based on $\mu$ CT .....	7
3.2. Acoustic properties with distance from jetted hole .....	12
3.3. Uniaxial Compressive Strength with distance to jetted hole.....	13
3.4. Fracture Toughness and Tensile Strength with distance to jetted hole.....	14
3.5. Comparing intact material with jetted in True-triaxial testing.....	15
<b>4. Discussion .....</b>	<b>18</b>
<b>5. Conclusion and recommendation.....</b>	<b>21</b>



## 1. Executive Summary

Based on the available material we come to the conclusion that jetting has no direct influence on the surrounding area. Analysis on multiple scales:  $\mu\text{m}$  (porosity); cm (mechanical and acoustical properties); dm scale (elastic properties with and without a jetted hole) do not show a significant changes compared to in-tact material, nor can a significant change be detected with respect to distance to a jetted hole. Results fall within the intra-block variability, and differences between blocks can be well explained by block-to-block variation.

True-triaxial elastic deformation tests have been designed and ran to test the effect of a lateral (jetted hole) on the elastic properties. The jetted hole itself was jetted with a rotating nozzle type, producing cylindrical holes. Comparing laboratory tests with a numerical model proved that the laboratory results may be well compared to a model with cylindrical hole embedded in a rock mass, much like a conventional borehole. The stress field around the jetted hole can therefore be well aproximated by the Kirsh-equations, modified for compression.

## 2. Laboratory Methods

### 2.1. Materials

To be able to analyse the effects of jetted holes, we had to use samples delivered by WP5. In practice this meant we focus on the rock types that were jettable at ambient conditions, with the technical knowledge of about twelve months into the project. The rock types used here are porous sandstones: “Gildehaus Sandstone” (project internal rock type code: SGH6-GI, IGSN: GFTRE0065) and “Friedewalder Sandstone” (project internal rock type code: SBS6-FR, IGSN: GFTRE0057). Intact material has been tested and showed initial porosities of 24.0 +/- 1.0% (Gildehaus) and 18.6 +/- 1.0% (Friedewalder). Both rock types were similar in mechanical properties: with ultimate compressive strength in the range of 40-60 MPa; Young’s moduli 9-15 GPa, Poisson’s ratios 0.2-0.3; and tensile strength 2-4 MPa. A more complete overview and analysis of physical properties will be presented in deliverable 4.1 (D4.1, due M36).

Intact rock material is compared to jetted material in three different types of analysis on different length scales, each requiring different sampling methods. For 3D microstructural analysis ( $\mu\text{m}$  scale) we studied cores (10 mm in diameter, approximately 90 mm long) drilled towards the jetted hole wall (i.e., with the core axis perpendicular to the axis of jetted hole itself), to see microstructural damage toward the jetted hole.

Often damage that cannot be recognized in microstructural analysis can have an effect on acoustic and mechanical properties. We therefore studied changes in acoustic and mechanical properties with distance of the jetted hole by core samples drilled with axis parallel to the jet-hole-axis, varying the axis-to-axis distance on a cm-scale (i.e., distance to jetted hole). In total 14 cores of 30 mm in diameter were drilled with axis-to-axis distances varying from 30-100 mm. Note that the jet-hole itself had a diameter of approximately 30 mm, and therefore the



minimum axis-to-axis distance was 30 mm. The total length of the cores varied between 180 and 240 mm. Of each core, 2 samples of approximately 75 mm length were prepared for compressive tests, according to a standard 2.5-1 length to diameter ratio (Paterson and Wong, 2005). The rest of the available core length was used to make disks of approximately 15 mm length, for Brazil Disk indirect tensile strength measurements, and fracture toughness (e.g., Guo et al., 1993), with a minimum of 2 samples per core.

Finally, to assess the bulk rock properties with and without a jetted hole, conventional tri-axial testing could not be used due to the dimensions of the provided jetted holes compared to sample size. We therefore use a true-triaxial apparatus capable of handling large samples: cubic samples of 300 mm x 300 mm x 300 mm (dm scale). Tests were performed on an in-tact block, and on a second block with a jetted hole running from the centre of one cube-face towards the opposing side (e.g., from  $\langle 150, 150, 0 \rangle$  to  $\langle 150, 150, 300 \rangle$ ).

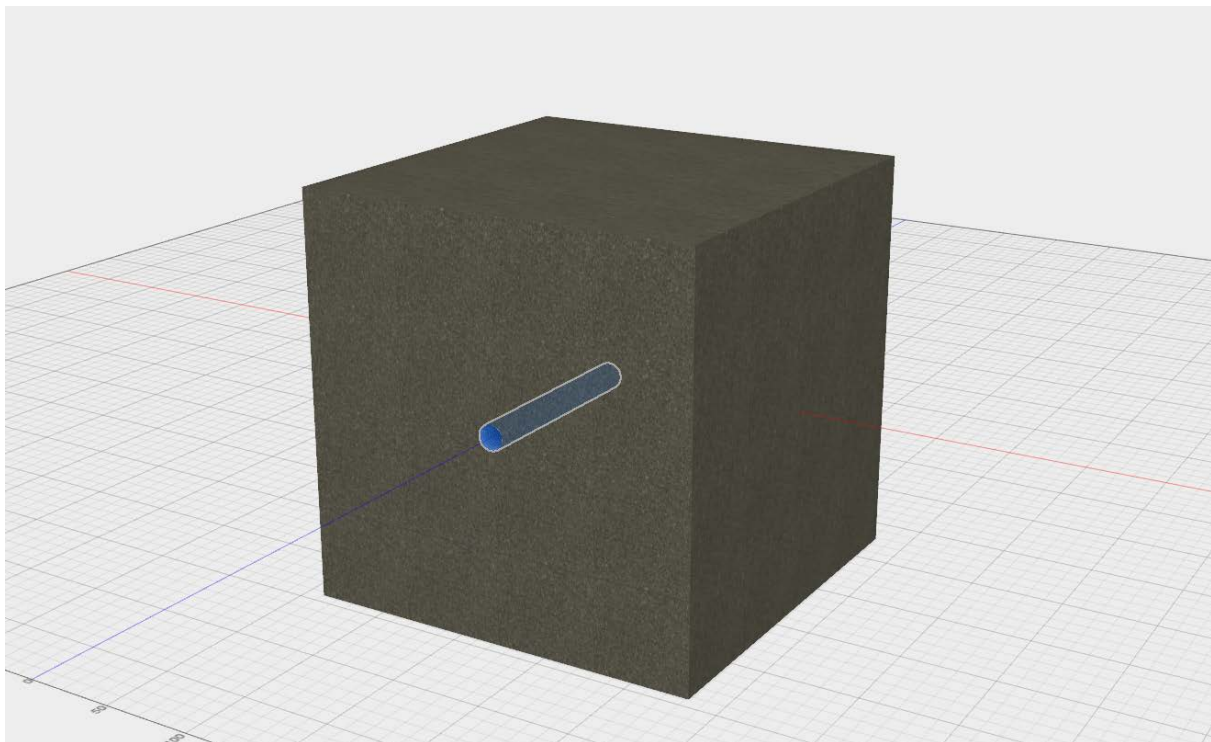


Figure 1, 3D rendering of a block with jetted hole (highlighted) in place, prepared for True-triaxial testing.

## 2.2. $\mu$ CT analysis

Three cores with a diameter of 10 mm were analysed using a Phoenix Nanotom - microCT & nanoCT Computed Tomography System as installed at the laboratory of TU Delft. The achieved resolution of the scan depends on the sample size, here the voxel size was 5.5  $\mu$ m. In post processing consecutive 2D slices of the reconstructed volume were analysed using a scripted image analysis routine (matlab). This routine analyses the porosity based on a gray-scale threshold within the sample area, for each image (see figure 1). This results in a



micrometer-scale resolution porosity profile. We focused on image-slices closest to the jet-hole, as well as a few cm away from the jet-hole wall for comparison.

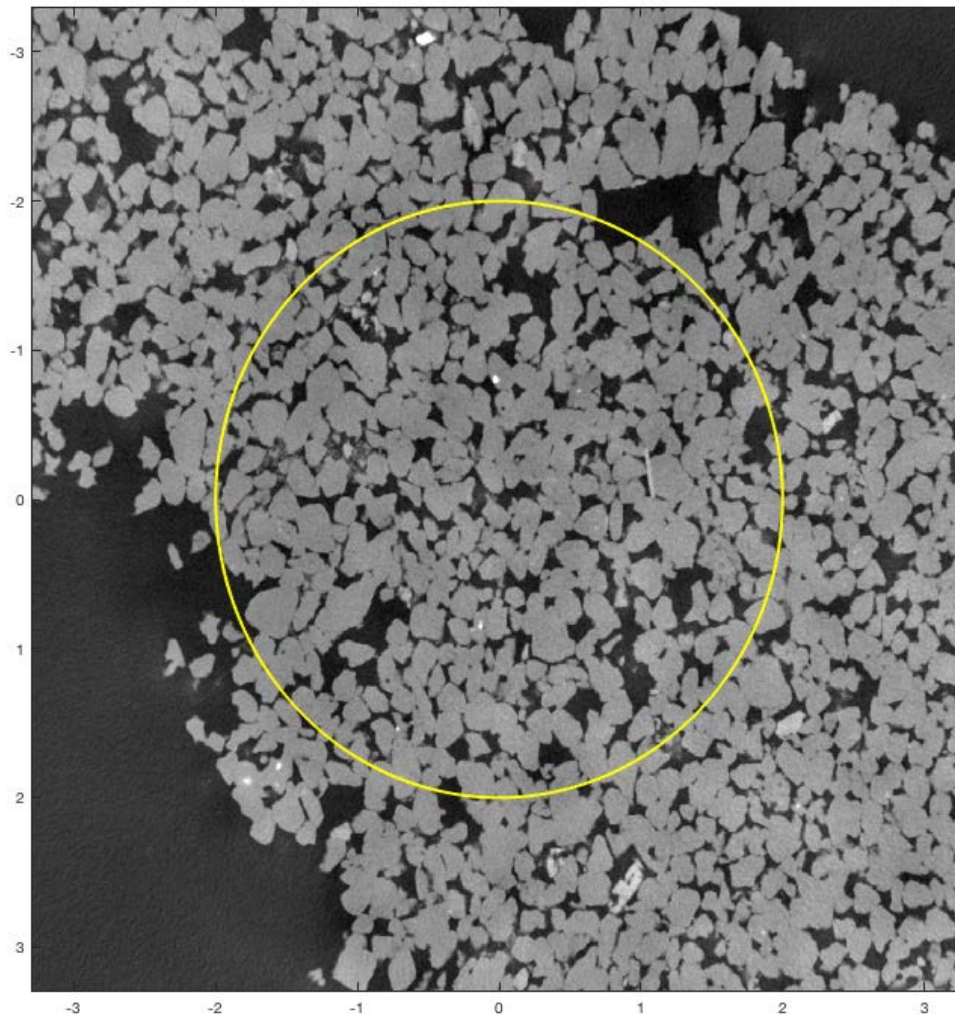


Figure 2, example of image slice with of a CT-scan with voxels (pixels in 2D) of 5.5  $\mu\text{m}$ . All pixels within the yellow circle are used to determine porosity. X and Y axis are in mm.

### 2.3. Acoustic wave speeds

Rock samples that were prepared for uniaxial strength testing were first used for non-destructive testing in the form of acoustic wave speeds. Transducers with peak frequency of 1 MHz were placed directly on the end-faces of the cylindrical samples, with coupling gel in



The SURE project has received funding from the European Union's Horizon 2020 research and innovation programme under grant agreement No 654662.

between, ensuring a good signal transfer. A single pulse of 1MHz was applied to the pulser, and picked up by the receiver, which in turn was connected to a high-speed acquisition oscilloscope (type: Yokogawa DLM4000). This procedure was repeated (at least 1000x) to obtain an average signal, limiting the effect of noise. We used both p-wave transducers (type: Panametrics, V103-RM), and s-wave transducers (type: Panametrics V153-RM). Arrival times were determined by analysing the stored signal in matlab, analysing both the waveform, as well as the spectrogram. The latter was primarily used for determining s-wave arrival, due to scattering of the p-wave that arrives earlier (see figure 2 for an example).

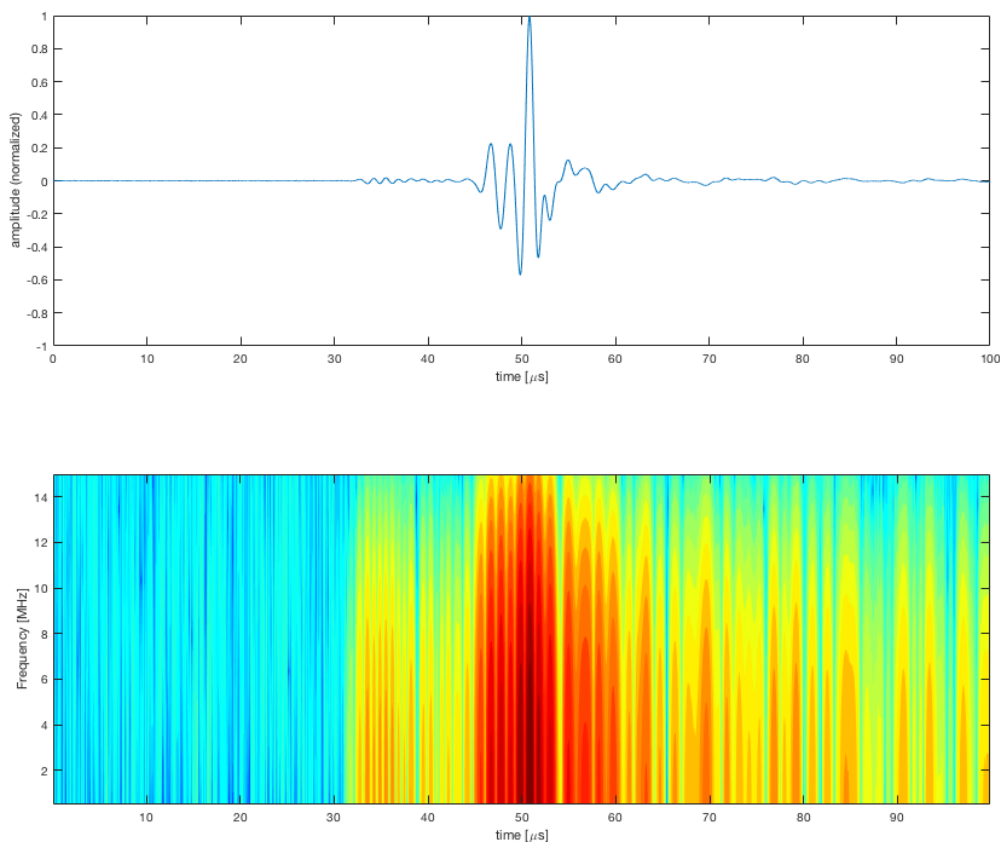


Figure 3, example of and s-wave arrival. Upper diagram: normalized waveform. Lower diagram, spectrogram of the signal, color range indicates qualitative signal strength from low (blue) to high (red)

#### 2.4. Uniaxial Compressive Strength

Static elastic properties and mechanical strength in compression was tested using stiff in-house built deformation apparatus, capable of handling load up to 500 kN. All samples were deformed at a constant displacement rate, resulting in an engineering strain rate of  $10^{-5} \text{ s}^{-1}$ ,



while measuring the resulting load. Axial displacement was measured continuously by two LVDTs. Radial displacement was measured by a chain-type LVDT (model MTS 815). Elastic properties were determined by evaluating the stress-strain curves in post processing, correcting for crack closure (initial part of the curve) and crack formation effects (close to failure).

## 2.5. Indirect Tensile Strength and Fracture Toughness tests

Tensile strength and Fracture Toughness were determined using the (modified) Brazil disk method (Guo et al., 1993). Tests were performed in an in-house built deformation apparatus, capable of handling axial load up to 50 kN, measured by a high-precision load cell (0.01 kN resolution). Displacement was measured by two LVDT's mounted parallel to the load direction. A constant displacement rate of 0.8  $\mu\text{m/s}$  was imposed such that failure would occur within a few minutes, which was determined by a calibration run in ramp-load mode.

## 2.6. True-triaxial tests

The true-triaxial deformation apparatus as installed in the TU Delft rock mechanics laboratory is able to handle large samples with loads up to 3500 tons, in three orthogonal directions (x, y, z). For samples of 300x300x300 mm this results in a maximum stress of 39 MPa. The experiment was conducted in four phases. During the entire run the displacement between two opposing sample faces was measured by two LVDTs per direction. In the first phase the samples were loaded hydrostatically to 30 MPa. In the second phase the load in y and z directions was kept constant at 1 MPa, while the load in x direction was increased to 20 MPa, such that lateral expansion due to the applied load could be measured. The third and fourth phases were similar to phase 2, but with different stress orientations (load in y, or z direction).

## 3. Results

### 3.1. Porosity analysis based on $\mu\text{CT}$

Porosity (fraction) measured by this method varied strongly between 0.12 and 0.26. A linear fit was attempted, but no statistically sound change in porosity could be determined in either of the three cores, in the closest to the jet hole wall (0-10 mm from jet hole wall). Although the linear fit is not statistically significant in all cases, a general upward trend is detected. For consistency the lower part of core 01 also checked for porosity changes along axis. The same general trend was observed.



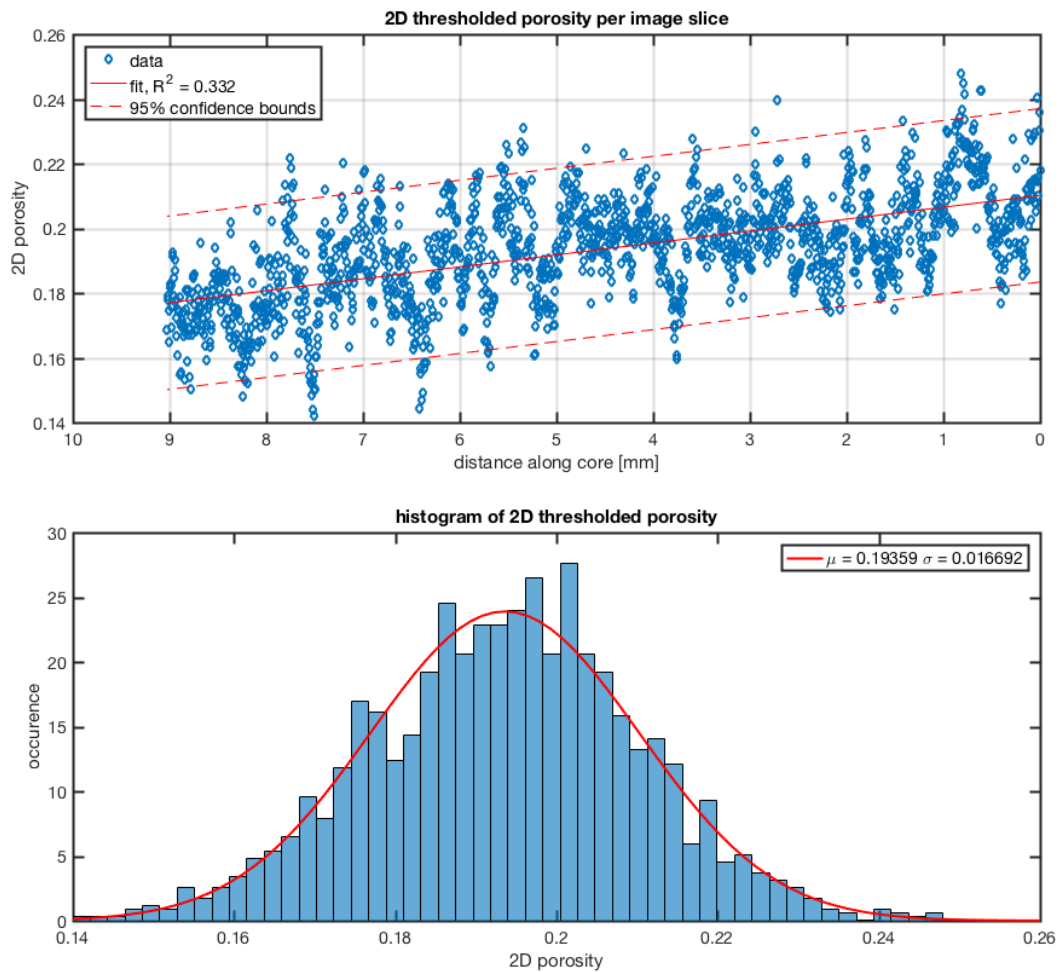


Figure 4, results from core GI\_J\_01, closest to the jetted hole wall. Upper diagram: porosity for each slice, fitted with a linear line. Lower diagram: histogram of the porosity distribution, fitted with a Gaussian curve.





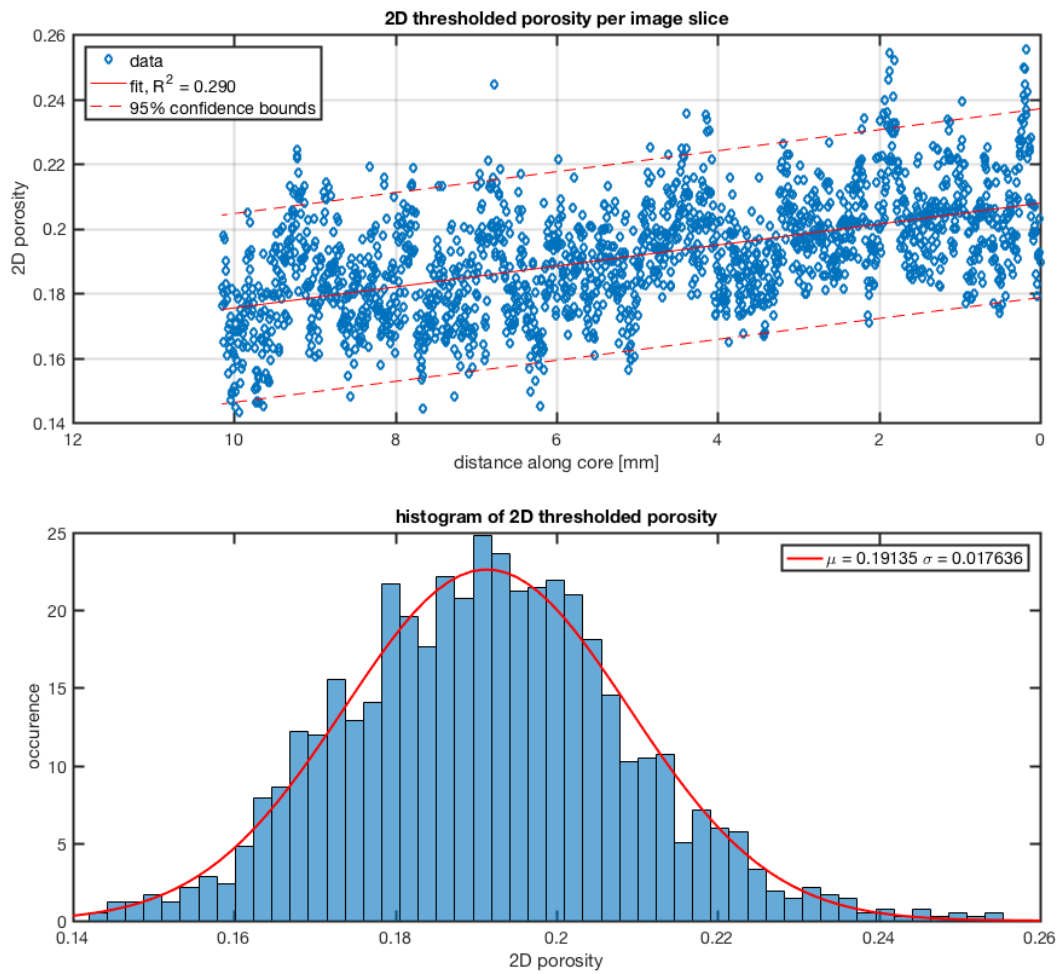


Figure 5, results from core GI\_J\_02, closest to the jetted hole wall. Upper diagram: porosity for each slice, fitted with a linear line. Lower diagram: histogram of the porosity distribution, fitted with a Gaussian curve.



Version 5/23/2019	Report on Stability of Laterals	page 10 / 21
-------------------	---------------------------------	--------------

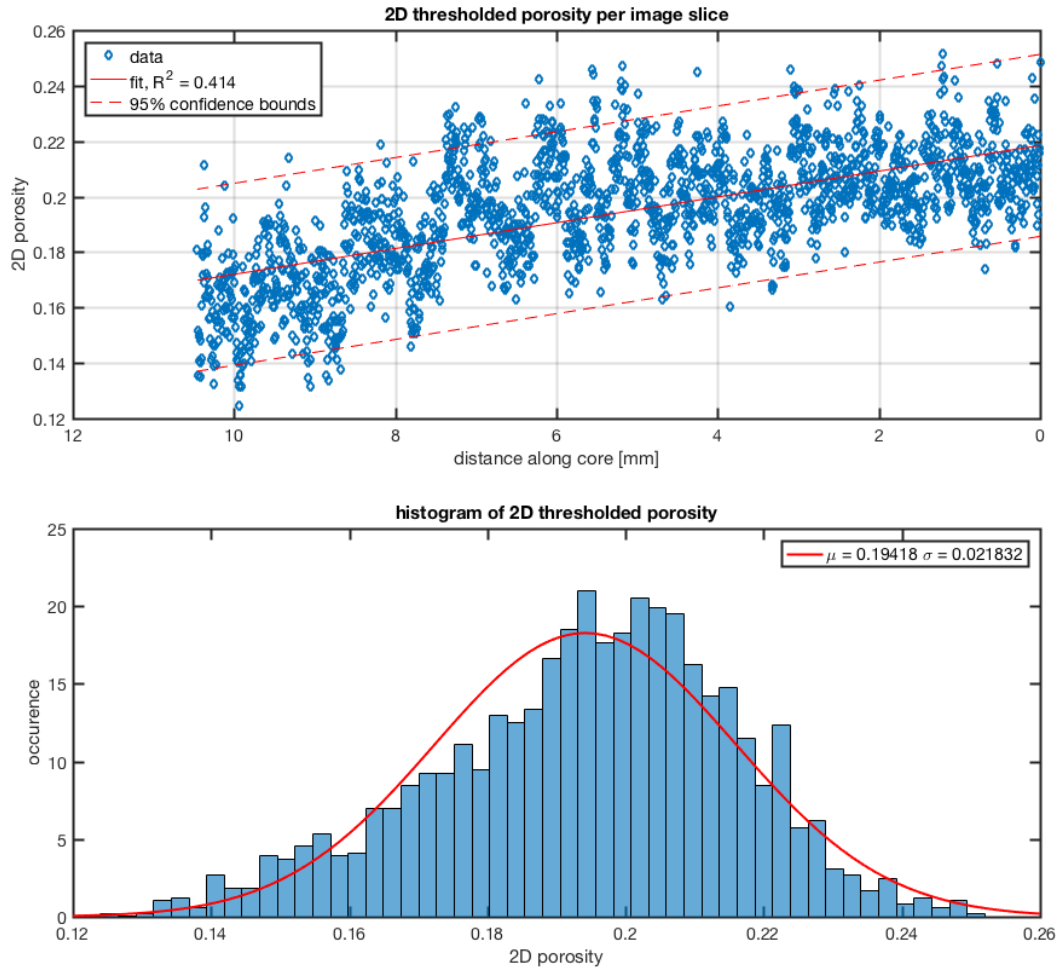


Figure 6, results from core GI\_J\_03, closest to the jetted hole wall. Upper diagram: porosity for each slice, fitted with a linear line. Lower diagram: histogram of the porosity distribution, fitted with a Gaussian curve.



Version 5/23/2019	Report on Stability of Laterals	page 11 / 21
-------------------	---------------------------------	--------------

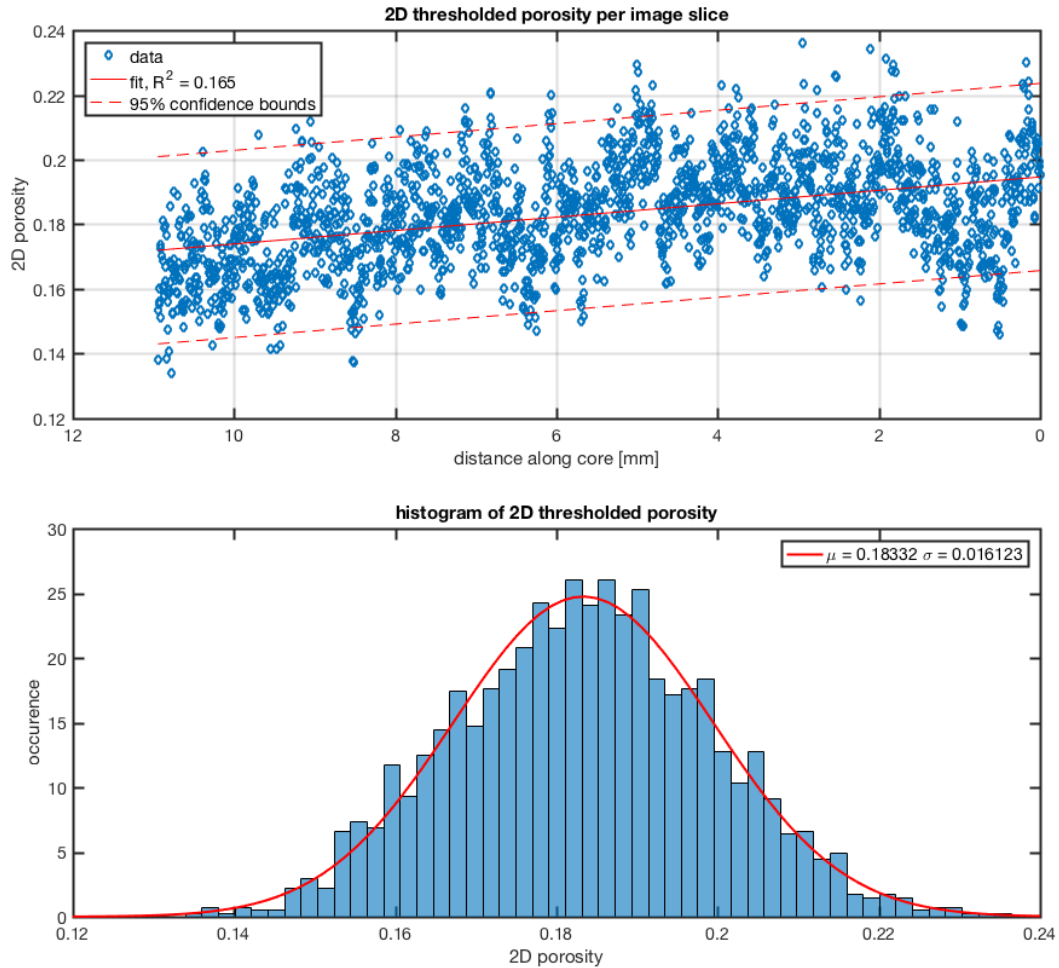


Figure 7, results from core GI\_J\_01, several cm away from the jetted hole wall. Upper diagram: porosity for each slice, fitted with a linear line. Lower diagram: histogram of the porosity distribution, fitted with a Gaussian curve.



Version 5/23/2019	Report on Stability of Laterals	page 12 / 21
-------------------	---------------------------------	--------------

### 3.2. Acoustic properties with distance from jetted hole

No significant changes in acoustic wave speeds with respect to distance to the jetted hole could be detected. Overall measured values range between 2.3 - 2.6 km/s ( $v_p$ ) and 1.6 - 1.8 km/s ( $v_s$ ). These are consistent with that of unjetted material ( $v_p = 2.61$  km/s and  $v_s = 1.75$  km/s, note that these are from a different block).

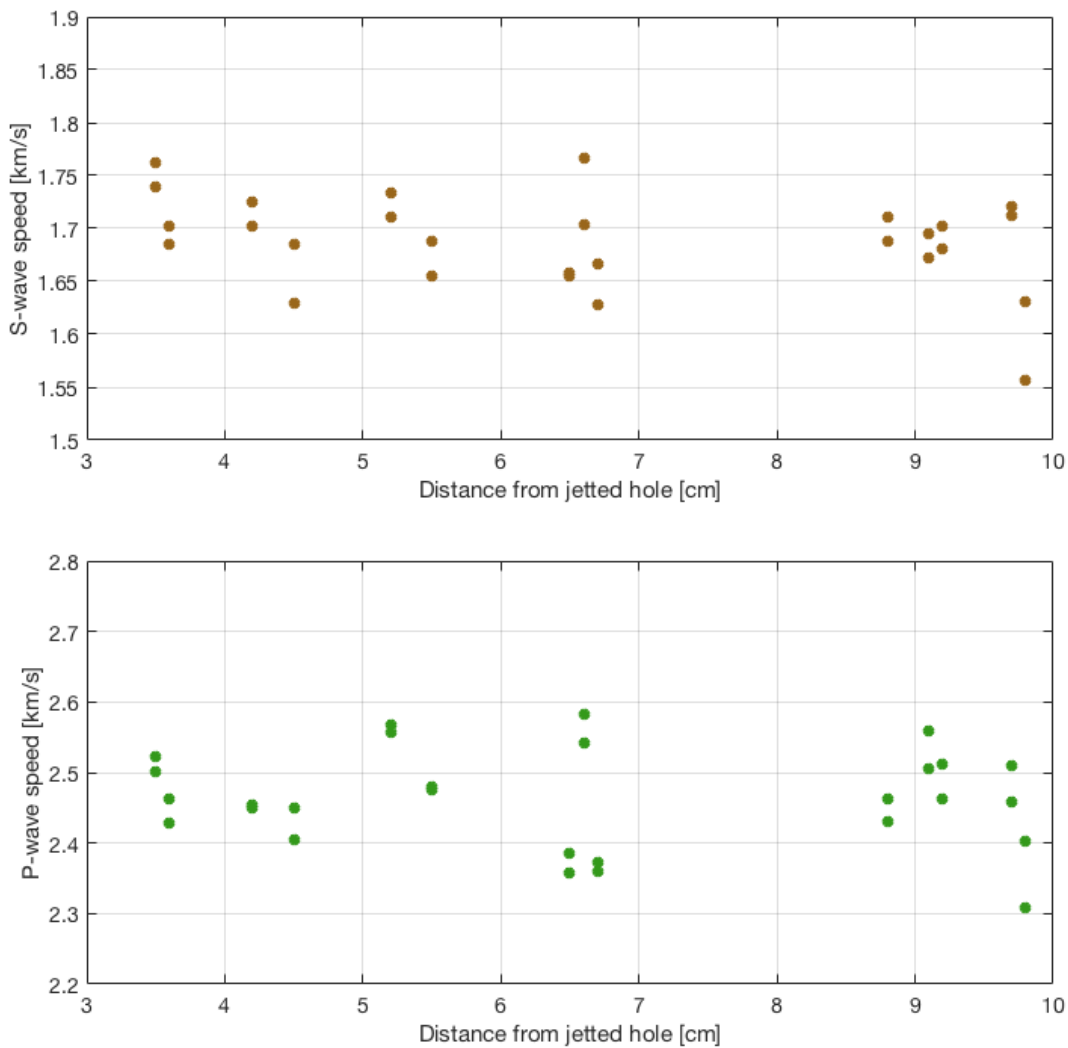


Figure 8, Acoustic wave speeds for cores, taken at a certain distance from a jetted hole (axis-to-axis). Upper diagram: s-wave speeds. Lower diagram: p-wave speeds.



Version 5/23/2019	Report on Stability of Laterals	page 13 / 21
-------------------	---------------------------------	--------------

### 3.3. Uniaxial Compressive Strength with distance to jetted hole

No significant changes in elastic properties or ultimate failure strength with respect to distance to the jetted hole was found. Ultimate failure strength results range between 13 - 38 MPa. Elastic properties range between 5 – 11 GPa (Young’s Modulus) and 0.06 – 0.32 (Poisson’s ratio). Samples with relatively lower rock strength can be associated with the lower end of values for elastic properties and vice versa.

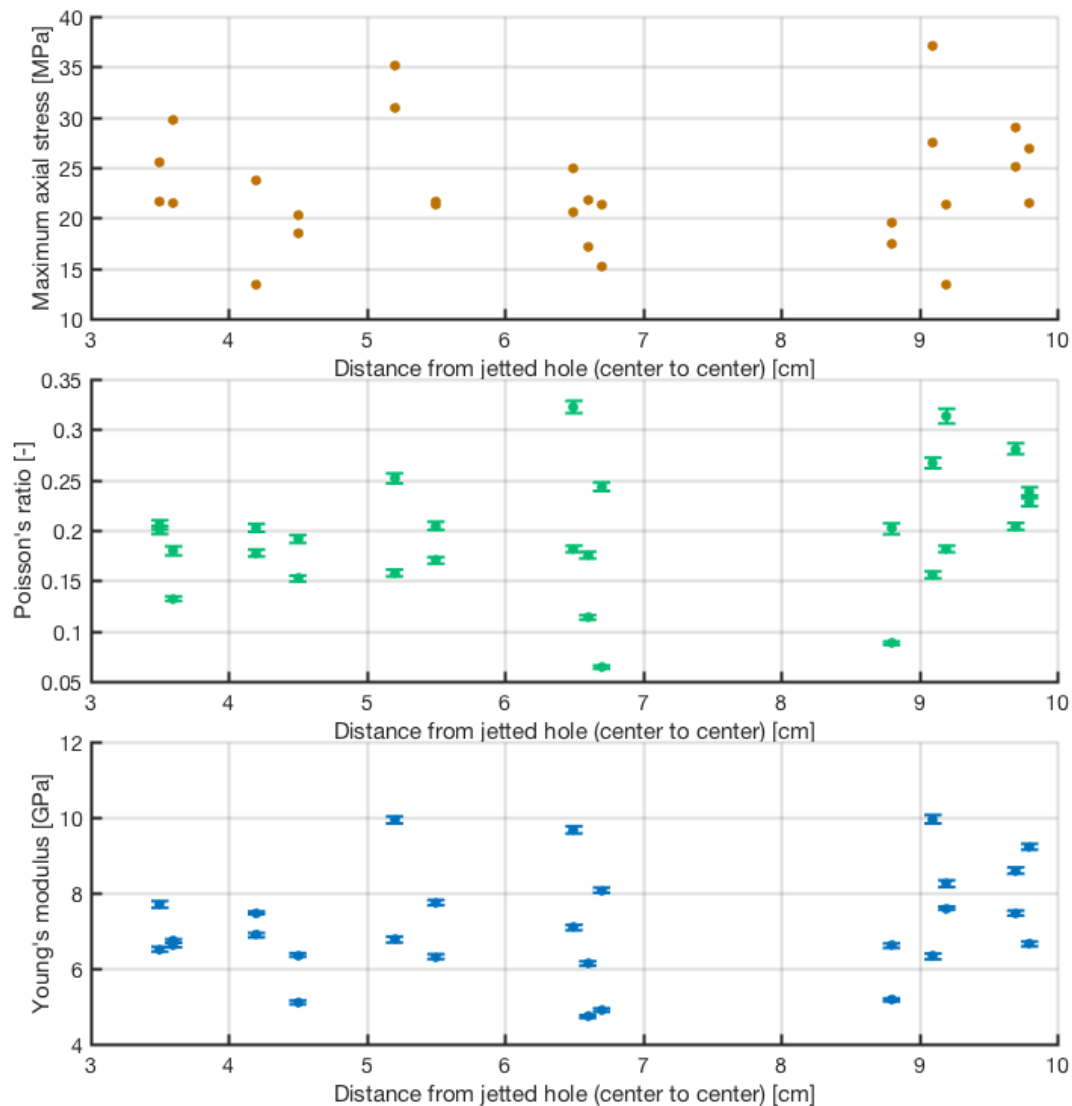


Figure 9, results of UCS tests on cores obtained at various distance of jetted hole. Upper diagram: peak stress at failure. Middle diagram: Poisson's ratio with error bars as 95% confidence interval of fit of the stress-strain (axial and radial) curves. Lower diagram: Young's moduli, error bars based on a 95% confidence interval of the stress-axial strain curve.



Version 5/23/2019	Report on Stability of Laterals	page 14 / 21
-------------------	---------------------------------	--------------

### 3.4. Fracture Toughness and Tensile Strength with distance to jetted hole

No significant changes in Fracture Toughness or Tensile Strength could be detected with respect to distance from the jetted hole. Fracture Toughness ( $K_{Ic}$ ) values range between 0.22 and 0.44 MPa $\sqrt{m}$ . Tensile strength values range between 1.4 and 3.2 MPa.

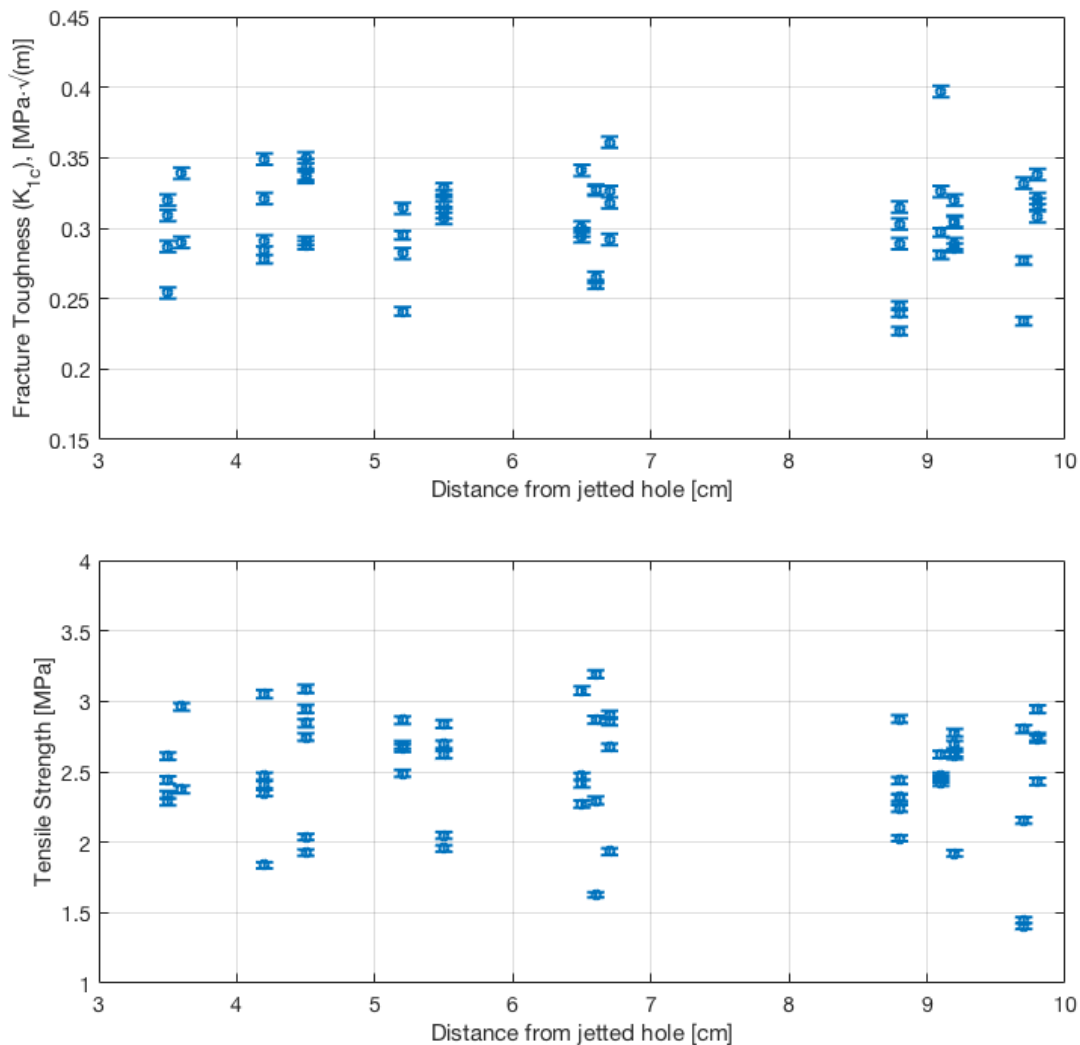


Figure 10, results of tensile tests on cores obtained at various distance of jetted hole. Upper diagram: Fracture Toughness. Lower diagram: Tensile Strength.



Version 5/23/2019	Report on Stability of Laterals	page 15 / 21
-------------------	---------------------------------	--------------

### 3.5. Comparing intact material with jetted in True-triaxial testing

Both intact and jetted blocks were subjected to the same loading phases, as indicated by the stress/time and strain/time graphs, shown in figure 11. For each phase, the elastic properties were determined from the stress-strain graphs (example is shown in figure 12). As can be seen in figures 11 and 12, the response was not perfectly elastic, as some creep effects are observed. For this reason, only the loading part of stress-strain graphs was used to determine the elastic properties.

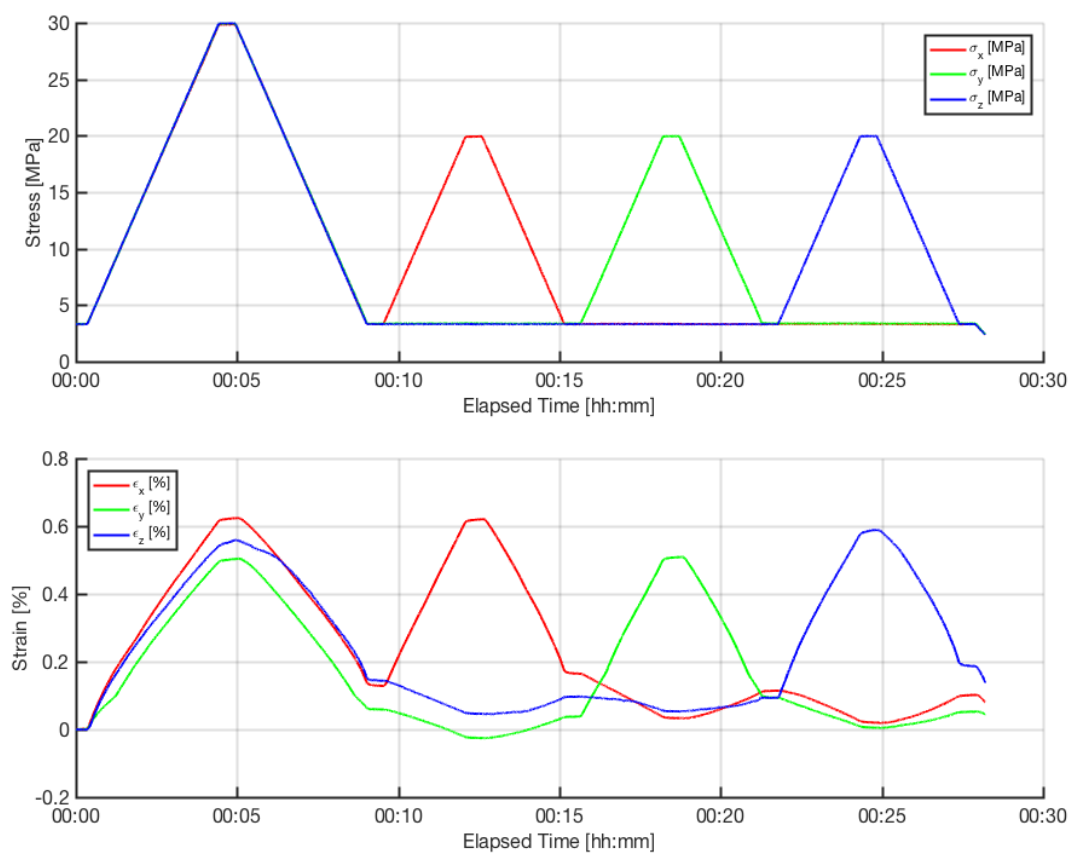


Figure 11, Upper diagram: applied load in 3 directions against time. Lower diagram: resulting strain against time. Results from test on block with jetted hole.



Version 5/23/2019	Report on Stability of Laterals	page 16 / 21
-------------------	---------------------------------	--------------

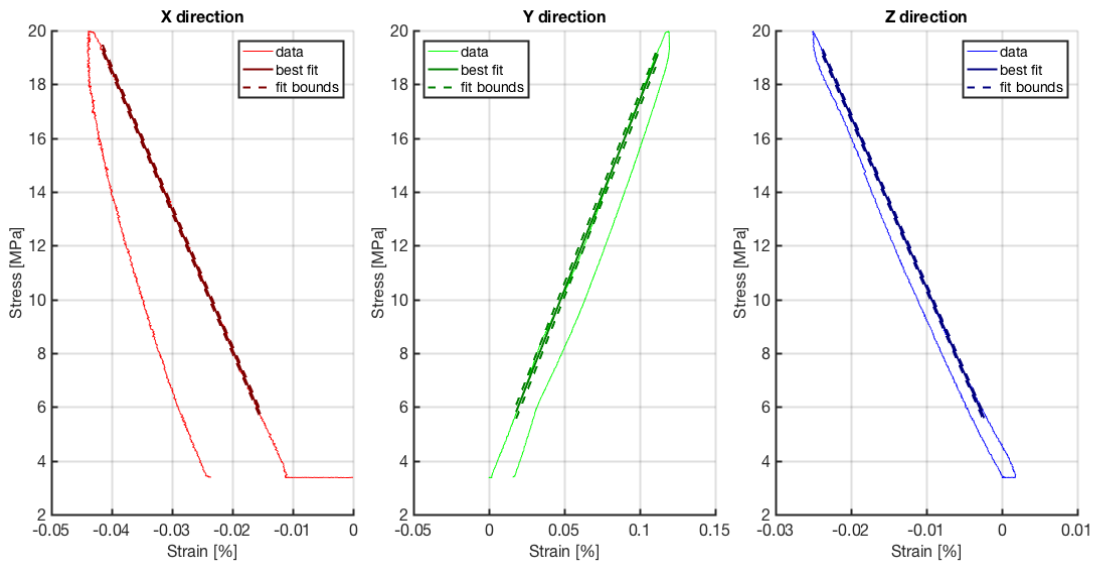


Figure 12, Example of determination of elastic properties, with load applied in y-direction (same as the axis of the jetted hole). X and Z-directions show lateral expansion as result of the applied stress in y direction. The slope of the best fits for all experiments is plotted in figure 13.





Version 5/23/2019	Report on Stability of Laterals	page 17 / 21
-------------------	---------------------------------	--------------

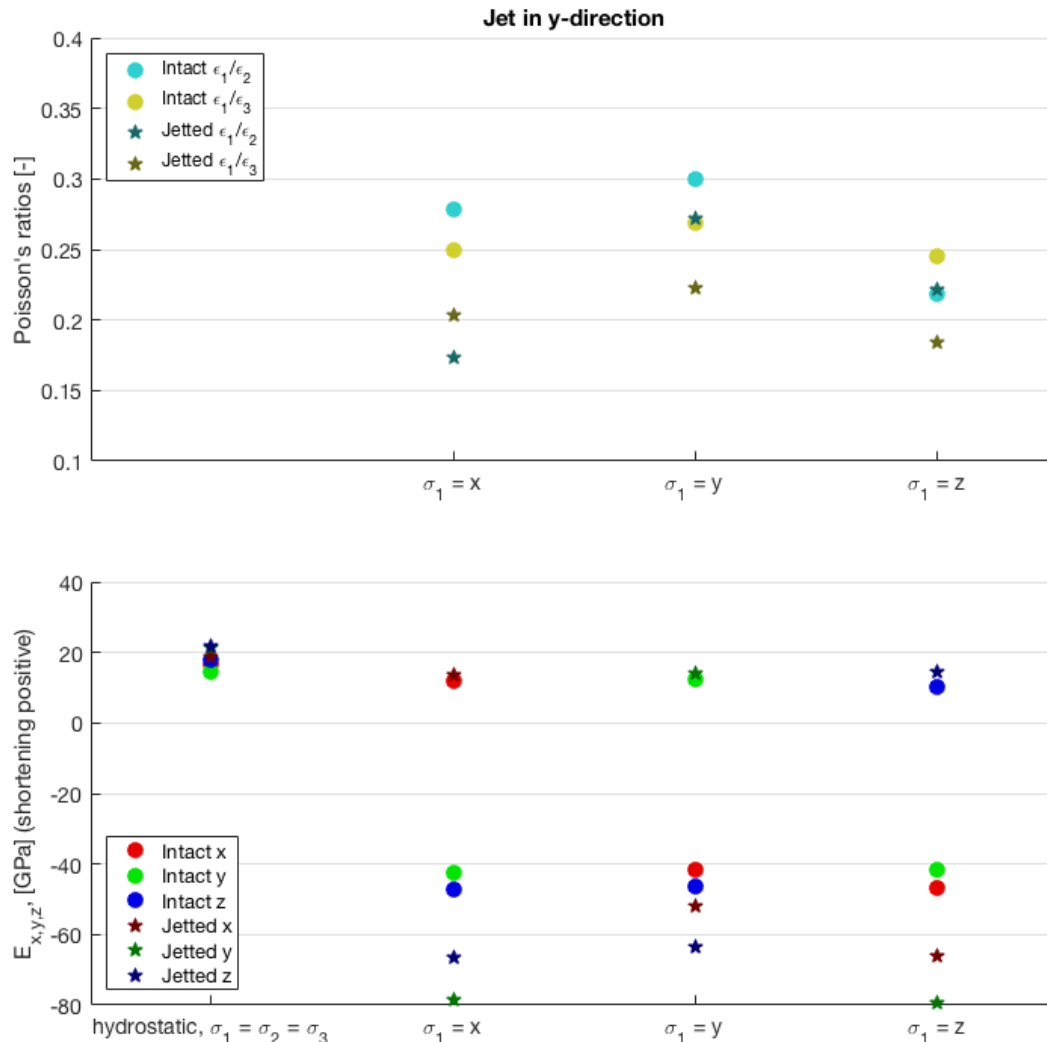


Figure 13, overview of elastic properties, grouped by experiment phase for intact and jetted samples.

Differences in measured elastic response during all phases is plotted in figure 13. We did not find significant changes in hydrostatic compaction of the blocks (first phase). For applied load in a single direction (i.e., phase 2, 3 and 4) some differences could be observed that are likely beyond that which can be explained by intra-sample variation. These differences are mainly in the lateral response to the applied load. With a jetted hole in place the lateral expansion less compared to intact material by a factor of roughly 1.5, as shown by the stiffer elastic responses (higher moduli). Possibly the some of the strain could be accounted for by deformation of the jetted hole itself.





Version 5/23/2019	Report on Stability of Laterals	page 18 / 21
-------------------	---------------------------------	--------------

#### 4. Discussion

- From the microCT-analysis, all samples seem to show an increase of porosity towards the jetted wall, that includes a lower part that was some 40 mm away from the jetted wall. However, the increase is not statistically significant based on the low poor fit ( $r^2$ -values) and is most likely due to a calculation artefact in the reconstruction of the raw-images to a 3D volume. Porosity averages are slightly lower compared to those measured by helium pycnometry on in-tact material, which falls in the range of 23.4 to 25.1%. The discrepancy can be explained by pores that are too small to be imaged by  $\mu$ CT analysis.
- First: the sampling material is not optimal, we are only able to discuss the results of a single rock type, which was the only rock type that was “jettable” under ambient (surface) conditions.
- From the cores drilled adjacent to the jetted hole (varying distance), no significant trends either of the following: acoustic wave speeds (both  $v_p$  &  $v_s$ ); elastic properties in compression, ultimate failure strength; tensile strength; and fracture toughness.
- Overall measured acoustic wave speeds of jetted samples slightly lower than that of unjetted material ( $v_p = 2.61$  km/s and  $v_s = 1.75$  km/s), which is most likely due to block-to-block variation.
- Assuming there is no trend with distance to the jetted hole, the data can be combined and the intra-block variation can be determined, given there are enough samples. This variation may be best described by the standard deviation of the data. If we then compare with in-tact material, we can see that the intra-block variability is similar for most properties (i.e., the width of the Gaussian curves in figure 13). Meter-scale variation from block to block (i.e., centres of Gaussian curves) can still exist due to slight differences in rock-type, for example as a result of different burial history.



Version 5/23/2019	Report on Stability of Laterals	page 19 / 21
-------------------	---------------------------------	--------------

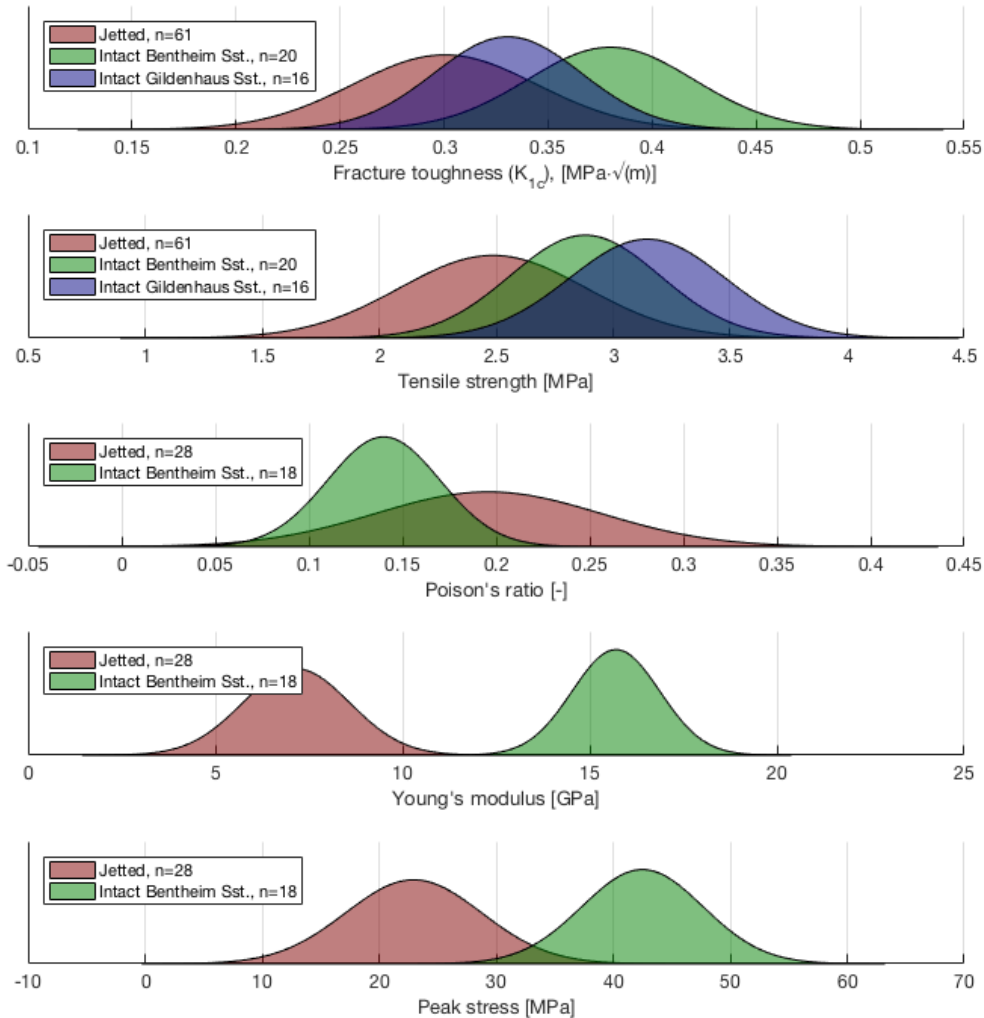


Figure 14, Gaussian distributions based on averages and standard deviations for intact rocks (both Bentheim Sst. and Gildehaus Sst.) compared to Jetted samples of Gildehaus Sst., assuming no variation with distance to jetted hole.

- This variability might also explain that the results of the true-triaxial tests are merely the result of block-to-block variation. The differences between the tests are not big enough such that they have to be explained by some other way, in this case damage due to a jetted hole.
- The observations in the true-triaxial tests can well be described by a cylindrical hole within a solid medium. The test was simulated within a numerical model (Comsol), showed similar results.



Version 5/23/2019	Report on Stability of Laterals	page 20 / 21
-------------------	---------------------------------	--------------

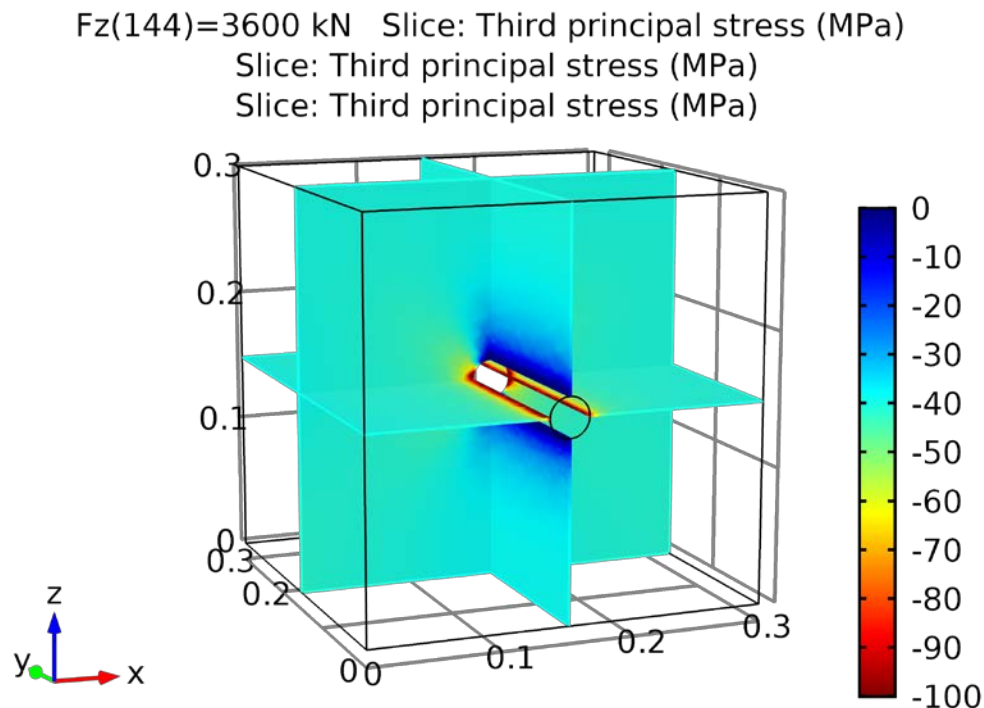


Figure 15, Result of a finite element model run, simulating the true-triaxial experiment. In this model run the stress/strain sign convention is inverse from the rest of this report, and negative numbers are compressive.

- It is hypothesized that jetting is easier when samples are subjected to a mechanical stress-field. We have therefore setup a new laboratory testing method to enable the jetting of rock-samples under true-triaxial stress. This might produce more appropriate samples and perhaps also other rock types.





Version 5/23/2019	Report on Stability of Laterals	page 21 / 21
-------------------	---------------------------------	-----------------

## 5. Conclusion and recommendation

Our results indicate that the emplacement of a jetted hole within a rock sample does not significantly alter the physical properties of the surrounding sandstone host-rock. Jetted holes themselves may best be modeled by a cylindrical hole within a solid medium.

Here, we have been comparing samples from different blocks, and argue that if jetting has an affect, it falls between the expected variability from block to block. This problem is unavoidable for core sampling-based testing, except if one drills into the exact same block.

That setup has been developed and will form the basis of future research.

When the radial jet drilling technology is sufficiently enhanced such that other rock types can be jetted, these can be tested along similar measurements as presented here.  $\mu$ CT analysis, acoustic wave speed tests and unconfined mechanical tests will be able to quickly assess if the jetted holes have had a significant effect in terms of (micromechanical) damage.

